Engineering Assessment Method for Anchorage in Corroded Reinforced Concrete

Mattias Blomfors, Kamyab Zandi

CBI Swedish Cement and Concrete Research Institute, Borås, Sweden

Karin Lundgren

Chalmers University of Technology, Gothenburg, Sweden

Oskar Larsson

Lund University, Lund

Dániel Honfi

SP Technical Research Institute of Sweden, Gothenburg, Sweden

Contact: mattias.blomfors@cbi.se

Abstract

There is an increasing need for reliable methods to assess load-carrying capacity and remaining service life of existing infrastructure. Several previous research projects have resulted in a verified, simple 1D model for assessment of anchorage in corroded reinforced concrete structures. Previous verification has involved both experiments and detailed 3D NLFE analyses. To further develop the 1D model it needs to be extended to comprise more practical situations. In order to facilitate an efficient extension procedure in the future, the size of 3D NLFE model that is required to capture the bond behaviour between corroded reinforcement and concrete is investigated. Beam-end models and models of sub-sections were studied, and the results in terms of bond stress and crack pattern were compared. Preliminary results indicate good agreement for some situations; however for some cases a section model seems to overestimate the capacity.

Keywords: corrosion, bond, concrete, reinforcement, nonlinear FEA

1 Introduction

Corrosion of steel reinforcement is the most common cause of deterioration in concrete bridges [1]. Many existing bridges are damaged with corrosion induced cracks or even spalling of concrete cover. Furthermore, the deterioration is believed to accelerate due to climate change thus more severe damage can be expected in the future [2]. The demand on load-carrying capacity of bridges is nevertheless increasing over time. There is therefore a growing need for reliable methods to assess the load-carrying capacity and remaining service-life of existing infrastructure.

Corrosion of reinforcement reduces the cross sectional area of reinforcing bars, and thereby their capacity and ductility. Furthermore, the volume expansion of corrosion products eventually cracks the concrete cover and adversely affects the bond between the reinforcement and concrete; this results in an inadequate anchorage capacity and may cause abrupt failure of the structure. The effect of corrosion on the bond capacity can be modelled using detailed three-dimensional nonlinear finite element (3D NLFE) models, e.g. [3]. These models are also capable of capturing cracking and spalling of the concrete, but wide practical applications are limited since 3D NLFE analyses require large resources in terms of time and competence.

In order to utilize the knowledge gained from previous research in engineering practice, there is

a need for simplified models and tools that are not only accurate enough, but are also time effective, for assessment of existing bridges.

1.1 Previous work

A simplified 1D model for the Assessment of anchorage in Corroded Reinforced Concrete structures (1D-ARC) has previously been established. It was originally formulated based on the analytical bond-slip model in Model Code 1990 [4] combined with a parametric study using 3D NLFE analyses [5]. The model has later been verified using test results of naturally corroded specimens [6], and validated by 3D NLFE analyses and experiments for high corrosion attacks leading to cover spalling [7].

The potential of the 1D-ARC model's practical use has been demonstrated in a pilot study of two bridges [8]. It was shown that for these two bridges only, the use of the 1D-ARC model reduced the costs by approx. 27 million SEK as unnecessary strengthening could be avoided. This exemplifies that use of this simplified model can result in enormous cost savings for society.

1.2 Approach

The previously mentioned case study [8] demonstrated great capabilities of the 1D-ARC model; however, it also revealed question marks for the model to be applied in practice. These question marks include applicability of the model on more realistic scenarios commonly seen in bridges compared to the ones often evacuated in laboratory test set-ups. For that reason it is aimed to validate or further develop the model for the influence of (i) multilayer reinforcement configuration, (ii) spacing between main bars and stirrups, as well as (iii) bundled and spliced bars.

In later stages of the work, physical, statistical and model uncertainties will be incorporated in the 1D-ARC model. The probabilistic 1D-ARC model will be constructed by using suitable distribution functions as inputs of the basic variables. Such a model will enable reliability evaluation of different structural elements and also probabilistic service-life prediction. Furthermore, it will also be used to quantify modification factors for the deterministic resistance model which enables a deterministic service-life prediction.

A parametric study of several cases is to be conducted; therefore it is important to make valid simplifications of the computational model to save modelling and computation time. The focus in this paper is put on choosing the level of detail of the 3D NLFE model needed to capture the bond behaviour in an anchorage region of a beam.

2 Studied beam geometry

In order for the assessment tool to be used in practice; it must be applicable to RC beam and slab types commonly seen in bridges. These include several parameters that can vary between structural members, e.g. reinforcement bar diameter, spacing between the reinforcement bars and concrete cover. Furthermore, the reinforcement bars can also be bundled, spliced, and placed in a multilayer configuration. Since corrosion attacks on structures in practice primarily depend on the environmental conditions (location, presence of chlorides etc.), and are not directly associated with the reinforcement layout, the number of situations to be considered in the extension of the 1D-ARC model is large.

The main goal of this paper is to investigate the level of detail required to capture the confining effects from surrounding concrete and stirrups on the bond capacity. Therefore, previously conducted physical tests and detailed 3D NLFE analyses [9] of a beam-end were compared to the results obtained from a smaller model of the same geometry.

The studied geometry has a square cross-section with 400 mm width and a main bar diameter of 20 mm. One main reinforcing bar is placed in each corner of the cross section with 30 mm concrete cover. An additional bar is placed between the bars in the bottom, giving a total of three bars to be tested for the anchorage capacity. Two out of three types of specimen, which have been subjected to laboratory testing, are included in this study: Type A without stirrups and Type B with 8 mm diameter stirrups with 44 mm spacing in the bonded zone. The bonded zone is 210 mm for both beam-end types; see Figure 1.
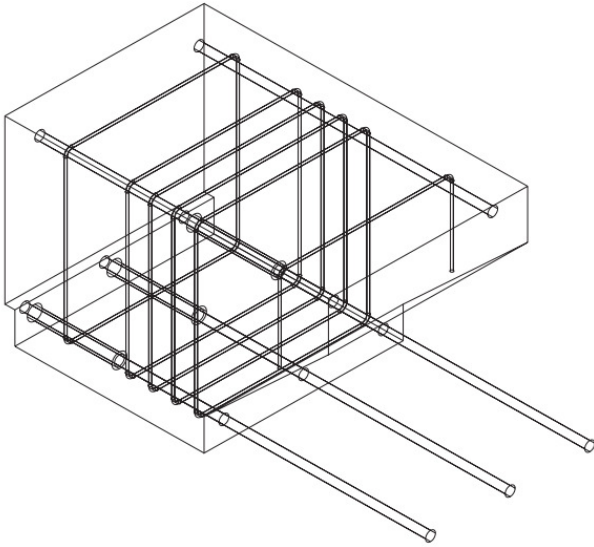
Figure 1: Type B specimen, Type A is similar but without stirrups in the bonded zone

The material parameters for the specimens were tested in [9]. The steel had a yield and ultimate strength of 510 and 610 MPa, respectively, and a Young's modulus of 200 GPa. The concrete properties, presented in Table 1, vary between the reference and the corroded specimens. This is due to the 3% sodium chloride content in the corroded specimens.

Table 1: Material properties of concrete and reinforcing steel (†, ‡ based on MC 1990 and EC 2 respectively)

Specimen	$f_{cc,cyl}$ [MPa]	F_{ctm} [MPa]	G_F † [N/m]	E_c ‡ [GPa]
Reference	27,7	2,2	61,2	28,7
Corroded	29,7	2,3	64,3	29,4

In the FE analyses, a corrosion level of 1,4% weight loss was applied to all bottom bars for the Type A specimen, while for Type B 1,7% was applied for the corner bars and 0,7% for the middle bar. It should be noted that the corrosion penetrations were larger for the physical experiments. The damage was however similar, this explained in more detail in [9].

3 Numerical modelling of anchorage

In this section the analytical bond model, 1D-ARC, is first presented. Then the bond model for the detailed 3D NLFE analyses is briefly explained. Two FE models of different complexity are thereafter presented; one consisting of only a section of the beam and another larger model of the beam-end region.

3.1 Description of bond models

3.1.1 Analytical 1D bond-slip model

The basic 1D-bond model in *fib* Model Code 1990 [4] forms the basis for the simple bond model for corroded rebar. Only an overview of the model is given here; it is fully described in [5].

The equilibrium equation along a reinforcement bar is

$$\frac{\pi \cdot d^2}{4} \cdot \frac{d\sigma}{dx} - \pi \cdot d \cdot \tau = 0 \qquad (1)$$

where d is the rebar diameter, σ is the stress in the rebar and τ is the bond stress. Elastic behaviour of the reinforcement is assumed, i.e. the stress follows Hooke's law. The bond stress τ is assumed to follow an elasto-plastic law

$$\tau = D(s - s_p) \qquad (2)$$

$$|\tau| \leq \tau_b(\kappa) \qquad (3)$$

where D is the bond stiffness, s is the slip, s_p is the plastic slip and τ_b is the bond strength which is a function of the hardening parameter κ. In case of corrosion, the hardening parameter is defined

$$\kappa = s_p + ax \qquad (4)$$

where a is parameter assumed to be constant and equal to 8,1, and x is the corrosion penetration. In case of corrosion this means a shift of the bond-slip curve in the slip direction. Physically, it can be explained by that the stresses and strains around a corroding bar has similar effects as those originating from pulling the bar.

3.1.2   Bond model for detailed 3D NLFE analyses

For the detailed analyses using three-dimensional solid elements the bond model is implemented through the use of interface elements between the reinforcement bar and the concrete. The model is capable of describing both the volumetric expansion of a rebar with the associated normal stresses when steel turns into rust, as well as the normal and bond stresses arising when pulling a corroded bar. A detailed presentation of the bond model for detailed 3D NLFE analyses can be found in [10-11].

3.2   Model set-up for detailed NLFE analyses

Two detailed 3D FE models of different sizes were set up in DIANA 9.6 [12] and will be presented in the following sub-sections. The first is a larger model of a beam-end region, while the second model is smaller and includes only a section of the beam. A symmetry condition around the vertical axis is used in both cases, reducing the model size to half.

For both models four node, three-side isoparametric solid tetrahedron elements, approximatively 10 mm in size, are used for the concrete and main reinforcement bars. The stirrups are included using embedded elements; this corresponds to full interaction between concrete and stirrups.

The entire circumferences of the main bars were corroded; non-uniform corrosion has been investigated in a previous study [7].

For concrete, a constitutive model based on nonlinear fracture mechanics using a smeared rotating crack model based on total strain was applied [13]. The crack band width was assumed to be equal to twice the element size which was later verified by studying the crack localizations in the analyses. The tensile softening of the concrete was modelled according to Hordijk [14] and the compressive behaviour according to Thorenfeldt *et al.* [15]. For the reinforcing steel an isotropic plastic model was used, together with a von Mises yield criterion. The equilibrium iterations were performed using a Quasi-Newton (BFGS) scheme together with a line search algorithm.

3.2.1   Beam-end model

The beam-end model and boundary conditions are depicted in Figure 2. The load is applied to the bars one at a time, by imposing a deformation on the nodes belonging to the rebar tip. The model is fully described in [9].
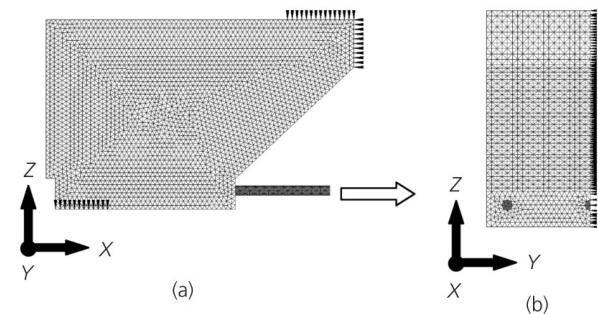

Figure 2: (a) side view, (b) front view of beam-end model

3.2.2   Section model

For the section model, part of the beam-end model is modelled separately. It consists of a 44 mm thick slice, i.e. the stirrup spacing, and the stirrup is placed in the center of the section. The width and height of the section model is 200 mm and 400 mm respectively, same as the beam-end. On one side of the section, the nodes belonging to the concrete are fixed in the pulling direction, and symmetry conditions are applied along the centreline of the section. Furthermore, displacement is prevented in the vertical direction in the centre of one of the bars. The section and the boundary conditions (BC's) are depicted in Figure 3.
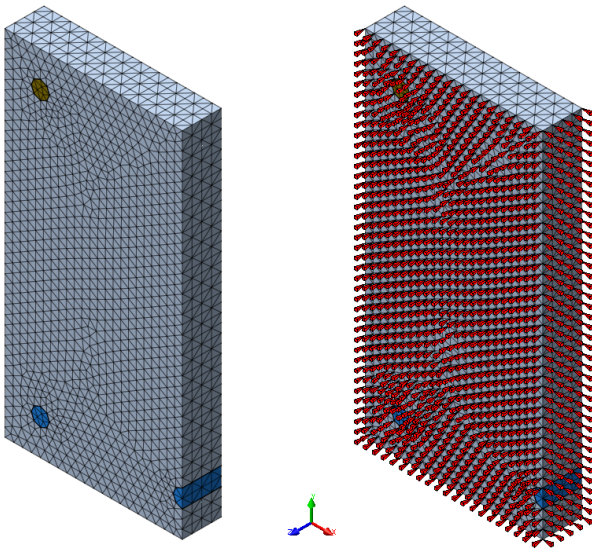
Figure 3: Section model (left), with BC's (right)

Analogous with the testing procedure and beam-end analysis, the bars are pulled one by one by applying an imposed deformation on all the end nodes of the pulled bar.

4   Results

Preliminary results from the nonlinear FE analyses of beam sections are presented together with those obtained in previous analyses and tests of beam-end specimens [9]. Bond stress curves and crack patterns are presented in the following.
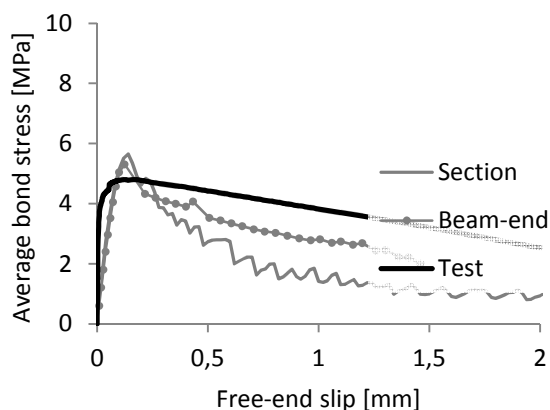
4.1   Bond stress curves

To compare the results from the two types of FE models and tests; the average bond stress versus imposed slip of the bar is presented. The average bond stress is for each load step calculated as the reaction force in the pulled nodes divided by the area over which the traction is acting, i.e. the rebar circumference times bonded length.

The results for the Type A and B reference specimens are presented in Figure 4-7 and the corroded cases in Figure 8-11.

Firstly, it is noted that corrosion reduced the maximum average bond stress for all beam-end analyses and tests. For the section analyses, the maximum average bond stress is only decreased for the corner bars. The middle bars are showing greater capacity when corroded.

Further, it is observed that for both Type A and B reference specimens the section model overestimates the capacity compared to the beam-end model and the test when the corner bar is pulled. However, when corroded, the section model agrees well with the beam-end and test values. Conversely, when the middle bar is studied the opposite behaviour is observed. That is, the results agree well for the reference case but are overestimated in the section analyses when corrosion is present.
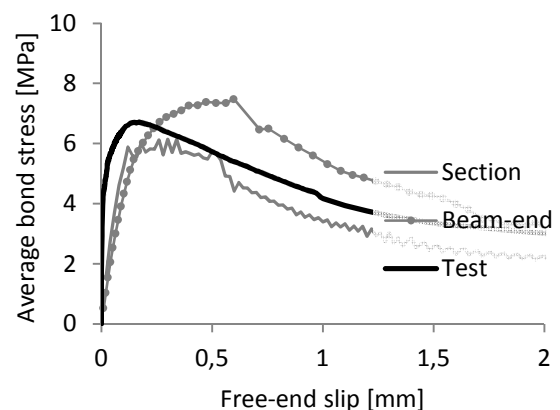

Figure 4: Type A - Reference: corner bar

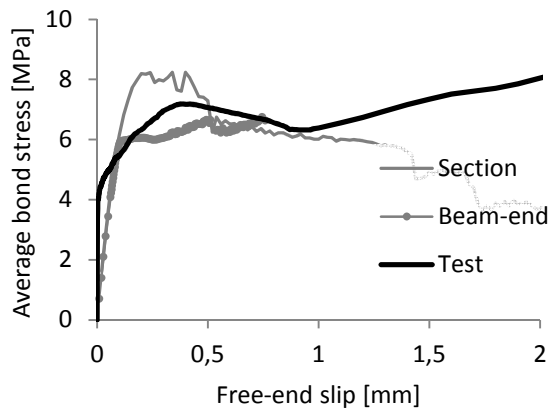*Figure 5: Type A - Reference: middle bar*

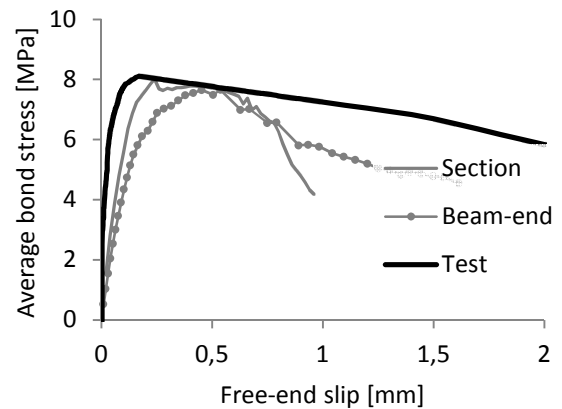*Figure 6: Type B - Reference: corner bar*

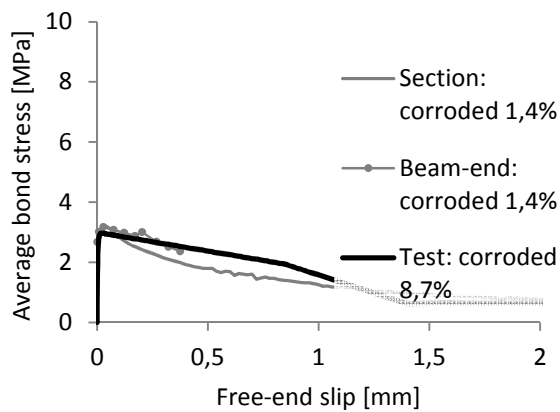*Figure 7: Type B - Reference: middle bar*

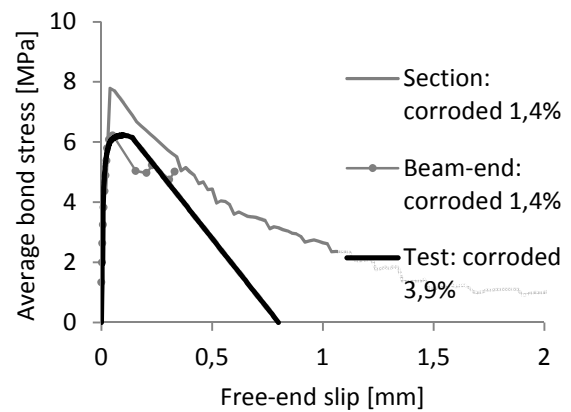*Figure 8: Type A - Corroded: corner bar*

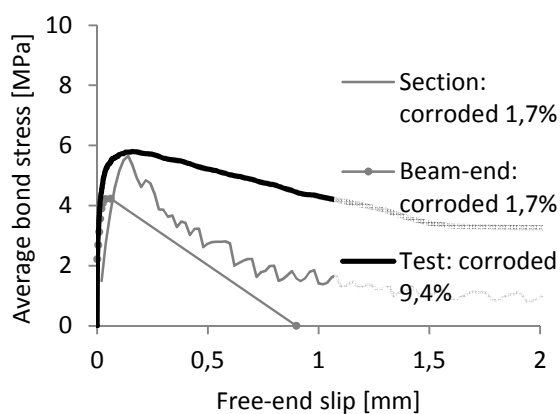*Figure 9: Type A - Corroded: middle bar*
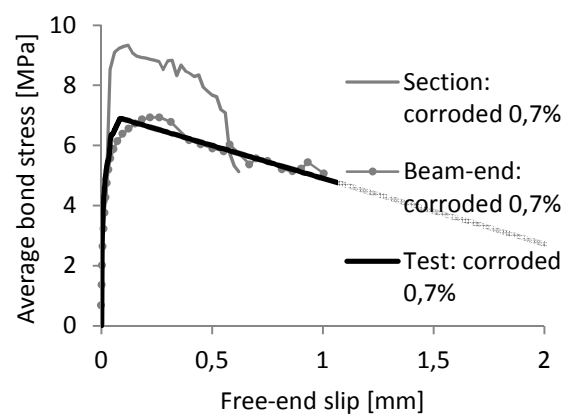

Figure 10: Type B - Corroded: corner bar

Figure 11: Type B - Corroded: middle bar

4.2 Crack patterns

The crack patterns obtained in the section analyses for Type A are shown in Figure 12. Red and blue color indicates one and zero ‰ in the first principal strain, respectively. The crack patterns were extracted for a slip level of 0,62 mm for both beam types for comparison. This was the last converged step for Type B when pulling the middle bar.

When the corrosion is applied, three cracks form around the corner bar. Four cracks form around the middle bar (three visible due to symmetry assumtion).
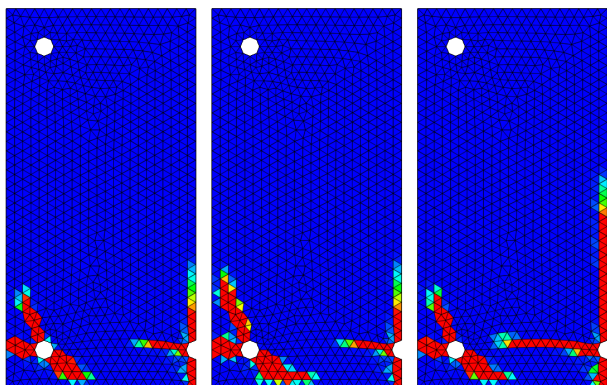

Figure 12: Type A crack pattern (from left: corrosion only, pull corner bar, pull middle bar)

The crack patterns for Type B are shown in Figure 13. When the corrosion is applied this specimen cracks less than the Type A. This can be explained by the confining effect of stirrups.
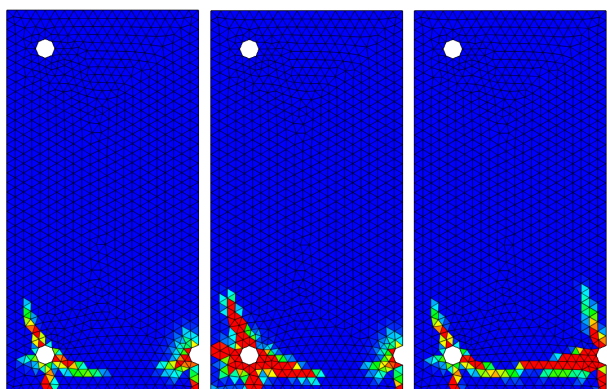

Figure 13: Type B crack pattern (from left: corrosion only, pull corner bar, pull middle bar)

Compared to the beam-end analyses, the crack pattern is similar except for the cracks propagating partly or entirely in the vertical direction. The inclined concrete surface of the beam-end, which thickens the concrete over the height of the specimen, hinders the cracks from propagating upwards. However some vertical cracks, or cracks inclined upwards, are present in the beam-end model. But when present, they are less pronounced in the beam-end model compared to the section model. It should also be noted that the magnitude of the crack widths after the corrosion phase appear to be smaller in the section model compared to the beam-end model for Type B specimens.

Furthermore, the crack patterns for the reference cases, when the uncorroded rebars are pulled, were checked and also regarded similar between the section and the beam-end analyses.

5 Discussion

The results agree reasonably well between the section model, the beam-end model and tests for most cases. However, for the corroded cases when the middle bars were pulled, the section model overestimated the bond capacity. Corrosion causes the maximum stress to occur at smaller slip levels; therefore smaller step sizes (0,001 and 0,005 mm/step) were investigated. The overestimation of average bond stress by the section model was however remained unsolved.

The FE analyses were performed using the same corrosion weight loss for the section model and the beam-end model. It was originally chosen to apply a corrosion which induced similar visible cracking in the beam-end analyses as in the experiments. The corrosion weight losses in the experiments were often greater than in the beam-end analyses. To investigate if the applied corrosion was too low in the section analyses, leading to excessive capacity, analyses with higher corrosion weight loss (i.e. 1,8% for Type B, middle bar) were carried out. Also for this level of corrosion, the bond capacity exceeded that of the beam-end and the physical test.

It is however believed that an adequate section model would simplify and speed up the advanced analyses required for the extension of the 1D-ARC model. Furthermore, a section model could also be used to study cases that are particularly hard to model. For instance, a beam-end model with

7

several layers of reinforcement experiences a large anchoring force and is prone to develop an unintended crack at the end of the anchorage length as the tensile capacity of the concrete is exceeded. Further, efforts will therefore be put towards refining the model and the solution strategy in order to obtain results on the safe side. It will also be investigated if a section model can be used for modelling a region of a beam with spliced reinforcement, a case of high interest in further development of the 1D-ARC model.

5.1   Conclusions

The following conclusions can be stated based on comparison of results from section analyses, beam-end analyses and experiments:

1) Without corrosion, the results were reasonably similar although the section analyses slightly overestimated the anchorage capacity of the corner bars;
2) With corrosion, the capacity agreed well for the corner bars, but the section model overestimated the anchorage capacity of the middle bars;
3) The crack patterns were similar in the section and beam-end analyses, as well as in the experiments.

6   References

[1]   Bell B. Sustainable Bridges D1.3 European Railway Bridge Problems. 2004. Available from www.sustainablebridges.net

[2]   Stewart M.G., Wang X., Nguyen, M.N. Climate change impact and risks of concrete infrastructure deterioration. *Eng Struct.* 2011; **33**(4): 1326-1337.

[3]   Coronelli D., Zandi Hanjari K., Lundgren K. Severely Corroded RC with Cover Cracking. *J Struct Engineering-ASCE.* 2013; **139**(2): 221-232.

[4]   CEB. CEB-FIP model code 1990. *Bulletin d'Information 213/214 CEB*. 1993.

[5]   Lundgren K., Kettil P., Zandi Hanjari K., Schlune H., Soto San Roman A. Analytical model for the bond-slip behaviour of corroded ribbed reinforcement. *Struct Infrastruct E.* 2012; **8**(12): 157-169.

[6]   Perez I., Tahershamsi M., Marí A.R., et al. 1D and 3D analysis of anchorage in naturally corroded specimens. Paper presented at: *Proceedings of the 10th fib International PhD symposium in Civil Engineering; 2014 Jul 21-23; Quebec, Canada*. 2014. p. 547-552.

[7]   Zandi K. Corrosion-induced spalling and anchorage capacity. *Struct Infrastruct E.* 2015; **11**(12): 1547-1564.

[8]   Lundgren K., Zandi Hanjari K., Nilsson U. A model for the anchorage of corroded reinforcement: validation and application. Paper presented at: *fib Symposium, Concrete - Innovation and Design; 2015 May 18-20; Copenhagen, Denmark.* 2015. p. 1-11.

[9]   Zandi Hanjari K., Lundgren K., Coronelli D. Bond capacity of severely corroded bars with corroded stirrups. *Mag Concrete Res.* 2011; **63**(11): 953-968.

[10]   Lundgren K. Bond between ribbed bars and concrete. Part 1: Modified model. *Mag Concrete Res*. 2005; **57**(7): 371-382.

[11]   Lundgren K. Bond between ribbed bars and concrete. Part 2: The effect of corrosion. *Mag Concrete Res*. 2005; **57**(7): 383-395.

[12]   TNO DIANA. FEM-software - release 9.6. Delft, The Netherlands. 2015.

[13]   TNO DIANA. DIANA finite element analysis user's manual - release 9.6. Delft, The Netherlands. 2015.

[14]   Hordijk D.A. Local approach to fatigue of concrete. PhD thesis, Delft University of Technology. Delft, The Netherlands. 1991.

[15]   Thorenfeldt E., Tomaszewicz A., Jensen J.J. Mechanical properties of high-strength concrete and applications in design. Paper presented at: *Conference on Utilization of High-strength Concrete*; *Stavanger, Norway*. 1987. p. 149-159.